Aerospace Science and Technology 124 (2022) 107514

Contents lists available at ScienceDirect

Aerospace Science and Technology

www.elsevier.com/locate/aescte

Multi-bubble scheme and structural analysis of a hypersonic stratospheric flight vehicle

Miguel Rodríguez-Segade *, Santiago Hernández, Jacobo Díaz

Structural Mechanics Group, School of Civil Engineering, Universidade da Coruña, Spain

ARTICLE INFO

Article history:
Received 8 September 2021
Received in revised form 14 January 2022
Accepted 22 March 2022
Available online 28 March 2022
Communicated by Saravanos Dimitris

Keywords:
Hypersonic vehicles
STRATOFLY
Multi-bubble configuration
Aircraft structures

ABSTRACT

The STRATOFLY MR3 vehicle is the main objective of the STRATOFLY project, which aims to develop a hypersonic air breathing concept capable of covering antipodal routes in less than three hours. The aircraft architecture features a waverider configuration, internally supported by multi-bubble integral cryogenic tanks hosting LH2 propellant, being one of the major challenges the integration of lightweight structures with the high-speed propulsion system. The objective of this research is to completely define an efficient structural scheme of the multi-bubble structures. To do so, a multidisciplinary analysis of the full-scale aircraft model is carried out to assess the viability of the vehicle prototype. Once the flaws of the initial structural layout are identified, a set of stiffener elements were developed to generate a scheme which can withstand the loads that hypersonic flight entails. In the multi-bubble structures, a topology optimization strategy was applied to obtain a set of tension rods connecting the top and bottom parts of the bubbles to support the pressure loads. The proposed configuration was sized and analyzed for multiple points of the aircraft mission, obtaining stress levels below the failure criteria adopted for each material. In addition, the results show low displacements that guarantee an adequate aerodynamic behavior and engine performance, while mantaining global natural frequencies in the range of commercial airplanes.

1. Introduction

The idea of reducing flight time drastically in long-haul, transoceanic flights has been constantly under development throughout last years, radically changing the concept of commercial aircraft.

The ideas of using hypersonic speeds (Mach $>$ 5), have been of interest to NASA and the USAF since the early 1950's, especially for space and military applications. In the recent years, hypersonics have captured great attention in the military, reaching a 3.6 billion in the US defense budget [1].

In terms of hypersonic effects, the vehicle experiences multiple phenomena simultaneously including aerodynamic shocks, aerothermal heating effects and aero-structural stresses. All these factors may influence the behavior of the vehicle, making critical a multidisciplinary design perspective [2].

Several programs have been developed throughout the world in the hypersonic field [3]. Recently, some prototypes have been successfully flown using scramjets, proving the viability of the concept. A scramjet (supersonic combustion ramjet) is a variant of a ramjet airbreathing jet engine in which combustion takes place in supersonic airflow. This allows the scramjet to operate efficiently at extremely high speeds. Some examples are the US X-43 Hyper-X [4], the X-51 [5], the Russian AJAX [6], and the Australian HyShot test aircraft [7].

Within the European area, more than a decade of research has been devoted to the development of hypersonic aircraft concepts: ATLLASI/II [8], LAPCAT MR2 [9], HIKARI [10], and HEXAFLY [11,12], and most recently, STRATOFLY [13], a project of stratospheric commercial airplane able to fly antipodal routes of about 20 000 km reaching hypersonic speeds, peaking at Mach 8, leading to three hour flights, thus creating a new scenery for long range itineraries [14]. The project is funded by the European Commission under the Horizon 2020 framework, and is a joint effort of research teams from many different countries: Germany, Italy, France, Belgium, The Netherlands, Spain and Sweden

* Corresponding author.
E-mail addresses: miguel.alonso1@udc.es (M. Rodríguez-Segade), hernandez@udc.es (S. Hernández), jacobo.diaz@udc.es (J. Díaz).

https://doi.org/10.1016/j.ast.2022.107514

Nomenclature

ATLLAS	Aero-Thermodynamic Loads on Lightweight Advanced Structures
AoA	Angle of Attack
ATR	Air Turbo Rocket
CAD	Computer-Aided Design
CFD	Computational Fluid Dynamics
CFRP	Carbon Fiber Reinforced Polymer
CMC	Ceramic Matrix Composite
CTE	Coefficient of Thermal Expansion
DFEM	Detailed Finite Element Model
DMR	Dual Mode Ramjet
EC	European Comission
ESA	European Space Agency
FE	Finite Element
FEA	Finite Element Analysis
FEM	Finite Element Method
FSD	Fully Stressed Design
GFEM	Global Finite Element Model
HEXAFLY	High-Speed Experimental Fly Vehicles
LAPCAT	Long-term Advanced Propulsion Concepts and Technologies
LH2	Liquid Hydrogen
NASA	National Aeronautics and Space Administration
OML	Outer Mold Line
SHEFEX	Sharp Edge Flight Experiment
TLR	Technology Readiness Level
TPS	Thermal Protection System
USAF	United States Air Force

The technical hurdles coming from the design of this disrupting vehicle require research and innovations in many scientific disciplines, and among them, the generation of a structural schemes able to support loads coming from many different sources like aerodynamic and thermal, also taking into account the performance in accordance to noise and emission regulations. Some studies have been performed to take into account these issues while designing hypersonic vehicles. Recently, Beachy et al. [15] proposed a neural network methodology including multi-fidelity data sets for designing the generic hypersonic vehicle model.

The first concept of the vehicle was designed by ESA [9], and consisted in a waverider configuration with the engine spanning the whole longitudinal dimension in a dorsal layout. This is considered as one of the most promising designs for wide-speed-range hypersonic vehicles [16,17]. A particularity with this design it is the use of its own shock-wave to generate extra lift in a high-pressure area, improving the lift to drag ratio.

Regarding the internal layout, a multi-bubble approach is used throughout the aircraft. Both the passenger cabin and the cryogenic tanks are designed as wide volumes where the skin forms a sequence of lobes, which are intended to work mainly under tension but have also relatively high inertia to resist global bending loads. This concept was introduced by Ardema [18–20], as an efficient way to design hypersonic vehicles. More recently the D8 double-bubble aircraft leverages this idea to obtain a wide body fuselage for a subsonic design. [21,22]. Furthermore, due to the large transverse dimensions of the blended wing body, a multi-bubble configuration is the only viable solution [23].

The propulsion system consists of a dual mode ramjet/scramjet (DMR) that operates between Mach 4.5 and Mach 8. Up to that speed, an air-turbo-rocket (ATR) is used as accelerator which has a dedicated flow-path integrated within the vehicle body [24]. Some research is under development regarding this type of engines [25], which could help to improve fuel consumption and range. In the STRATOFLY vehicle, the inlet concept is based on the XB-70 configuration [26] but with an inward turning conical air intake. The nozzle contour was designed using the Method of Characteristics (MOC) and consists of an initial 2D isentropic expansion followed by a 3D isentropic expansion. At high speeds, the air residence time within the engine is very low, in the order of milliseconds, so fuel mixing becomes a key issue [27]. In addition, the development of an efficient flame stabilization process is of vital importance for the performance of the propulsion system [28]. In this case, a vertical strut layout allows for good mixing and combustion efficiency. Due to the size of the vehicle (almost 100 m), the engine has to be highly integrated within the airframe. From a structural point of view, the engine has very demanding requirements concerning the overall stiffness, as local deformations could render the scramjet unusable. For that reason, a lightweight structural layout that bonds together the skin, engine, passengers cabin and tanks is of paramount importance and one of the main objectives of this work.

The contribution of this research consists in the definition of the structural scheme of the vehicle, according to the fixed configuration of the waverider, propulsive paths and cryogenic tanks layout. To do so, the multi-bubble concept will be assessed, incorporating the required additional components capable of stiffening the structure, achieving a better global behavior under a set of multidisciplinary loads. For that purpose, a high fidelity Global Finite Element model (GFEM) was developed to predict the overall response of the STRATOFLY vehicle in its multiple flight conditions, as well as to assess the efficiency of the selected structural solutions. That model could be used in further studies to perform Multidisciplinary Design Optimization (MDO) and obtain improved designs. This approach has been used previously in the design of hypersonic vehicles [29,30]. However, the structural mass models are predicted using analytical approximations. Therefore, the inclusion of a full-scale FEM model within a MDO framework could enhance the designed configuration and vehicle performance.

This paper is structured in the following sections. In Section 2, a general overview of the vehicle characteristics is firstly introduced and the conceptual design is presented. Based on the geometry of the conceptual design, a initial Finite Element (FE) model is elaborated in Section 3, performing an structural analysis that will expose the flaws and shortcomings of the preliminary design. To overcome these deficiencies, a structural scheme is proposed in Section 4, including structural elements such as stress relievers, bubble tension rods and lightweight connecting elements. The results are presented in Section 5 and finally, Section 6 offers the concluding remarks.

2. STRATOFLY vehicle configuration

The STRATOFLY MR3 vehicle is an horizontal take-off air-breathing concept. As explained before, the propulsion system includes a DMR and a ATR as accelerator, both highly integrated with the multi-bubble tanks and passenger cabin. The ambitious aim of providing transport for more than 300 passenger requires a big passenger cabin, that should be accommodated alongside the large volumes of cryogenic tanks that contain the needed propellant. The general dimensions are 94 m length, 41 m wing span with a total height of 17 m, resulting on an approximate overall volume of 10 000 m^3. Fig. 1 presents the general dimensions of the vehicle alongside, three transverse sections that show the internal tanks (line pattern), passenger cabin (light blue) and engine ducts.

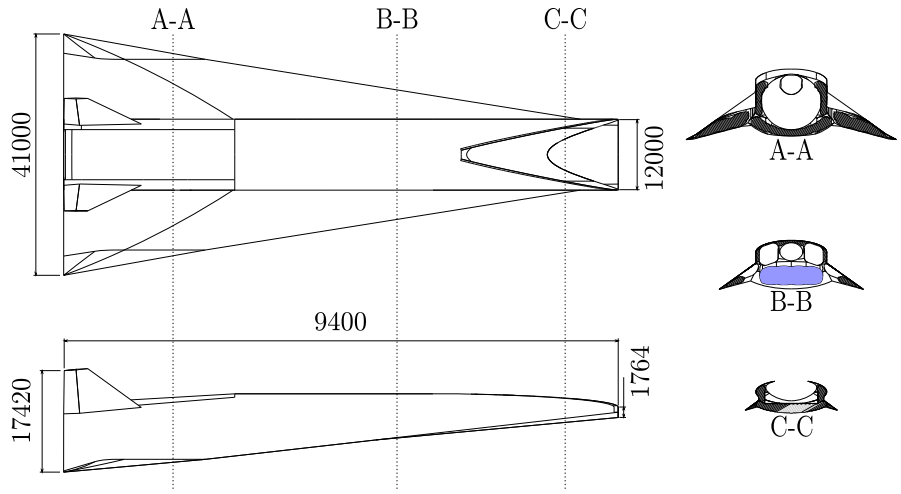

Fig. 1. Stratofly dimensions in mm and section views. (For interpretation of the colors in the figure(s), the reader is referred to the web version of this article.)

The waverider configuration with a dorsal engine layout was designed by Murray et al. [31] after several optimization cycles. They employed the osculating cone solution developed by Sobieczky [32], to obtain a Mach 8 waverider with a modified delta wing to improve performance in sub- and transonic flight. To achieve the STRATOFLY MR3 vehicle mission, it was necessary to expand its waverider internal volume to allow for a 300-passengers cabin. New techniques are being developed to obtain more efficient configurations. In this trend, Zhang et al. [33] achieved full waverider design that provide sufficient space for the engine and large payloads.

The arrangement of the body of the vehicle follows an integral tank architecture, which means that the volumes designed to host the propellant contribute to the general resistant scheme. Overall, this approach achieves high inertia values and thus, low displacements compared to those obtained in commercial aircraft wing tips. The main disadvantages when implementing this concept are that the tanks undergo large volume changes during fuel filling and depletion, subjecting the surrounding structures to demanding actions. For this reason, the insulation system is key to the success of the vehicle operation.

As mentioned, the cryogenic tanks distribution is designed to provide inertia and maximum fuel capacity. They can be classified as DMR tanks, which surround the engine; wing tanks, located below the wings; front tanks, between the inlet and passenger cabin and rear tanks, which are below the engine nozzle. Choosing an efficient shape and position of the bubbles supposes an engineering challenge, as the curvature of the lobes, the position of the cusps and the total volume greatly influences not only the behavior of the tank structure, but also the complete vehicle response to the loads.

Hydrogen is the fuel selected, given its high specific energy content, which is necessary to cover long distances. However, a storage method to increase its density is required to make it practical for hypersonic applications. Conventional solutions are as a compressed gas or as a cryogenic liquid. Liquid hydrogen is chosen for requiring less weight and smaller volume [34], but the low temperature requirements imply the need of a thermal protection system to insulate it from the remaining parts of the aircraft.

High aerothermodynamic heating can pose formidable challenges for structure development, which must be addressed through a combination of effective thermal management approaches and structurally efficient designs to achieve viable vehicles. As a mean to sustain the high temperatures imposed by the hypersonic flight regime in the order of 2500 K, the design of an efficient thermal management system is of paramount importance [35]. Three approaches can be considered: using a thermal protection system (TPS), actively cooling the structure or using a hot airframe from materials that can withstand the hypersonic environment. Although using a thermal protection system is the most mature technology, it is not the most efficient, as it adds parasitic weight which does not provide structural capacity. For this aircraft, a combination of heat pipes in the leading edges, hot structure in the fuselage body and wings, and active cooling on the most demanding areas of the engine are employed. While selecting the materials to be used, special attention must be taken to control the effects of coefficient of thermal expansion (CTE) mismatch, which produces high deformations, as was shown in the SHEFEX I Flight experiment [36].

3. Preliminary model

The starting point of the work is the computer aided design (CAD) model of the vehicle [37], which defines the position of all the components of the aircraft. The prototype is an evolution of the LAPCAT MR2.4 [38] vehicle, with four main modifications: a streamlined design for the passenger cabin, a fully closed DMR nozzle and exterior skin, the removal of the canard surfaces and a cryogenic tank configuration adapted to this modifications.

A brief description of the main parts included in the CAD assembly shown in Fig. 2 is presented below:

- Exterior skin: Defines the OML (Outer Mold Line) that fully covers the whole vehicle with a smooth surface to obtain good aerodynamic performance.
- High speed propulsion system: Provides the thrust needed to complete the mission.
- Passenger cabin: Hosts the passenger, crew, luggage and general systems and equipments.
- Cryogenic fuel tanks: Contain the LH2 needed by the engine at the correct temperature and pressure.
- Empennages: Vertical elements that provide lateral-directional stability during flight.

Using the CAD model as a starting point, we developed a GFEM including the necessary structural configurations. This was one of the first milestones, as it allowed to assess the feasibility of the architecture designed. Its purpose was to provide a baseline design, featuring all the relevant components of the aircraft, and to provide sufficiently accurate results to evaluate the general performance in the most critical scenarios.

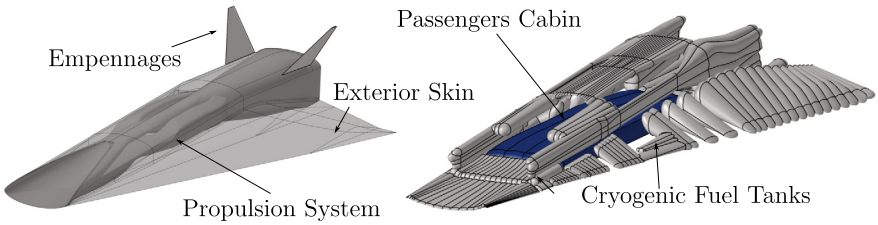

Fig. 2. General layout and multi-bubble distribution of the STRATOFLY MR3 vehicle.

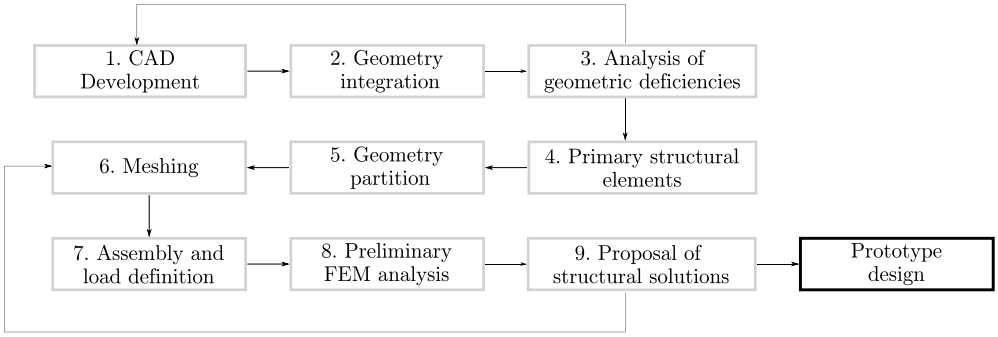

Fig. 3. Flowchart of the design analysis process.

3.1. Methodology and assumptions

Given the complex geometry of the model, it was necessary to perform a precise geometry cleanup and partition to guide the discretization algorithm that was later applied. The complete flowchart of the procedure is depicted in Fig. 3. The major structural components have been meshed using linear shell elements, membrane-bending isoparametric with 6 degrees of freedom per node, using Altair's Hyperworks pre-processor, Hypermesh [39]. A quad-dominated approach has been pursued throughout the entire assembly, refining the element size in areas with high curvature or complicated topology.

To model the connections between neighboring parts of the assembly a glued contact or tie interaction is used. This interaction is defined as a special type of linear contact model which imposes the condition that there is no relative, normal or tangential motion between the contacting surfaces. The advantage of using this technique is that no detailed structural elements are needed at the interface between the two contacting surfaces, which belong to a higher TLR (Technology Readiness Level). This is relevant because in the current structural configuration, the multi-bubble tanks are part of the structural support of adjacent components. In a detailed model, this connection requires a compatible mesh and additional elements to ensure complete structural and thermal bonding between the materials. The potential inaccuracy associated to this approach only affects locally, but the effect can be considered negligible further away from the area. This accurately predicts the behavior from a global perspective, easily allowing detailed simulations, including frames, stringers and fasteners in further studies. In Fig. 4, the bonded surfaces between the DMR and the cryogenic tanks are highlighted in grey color.

As we need to study the aircraft during flight, displacement boundary conditions can not be imposed over the structure. To carry out a static analysis in this kind of situation, the inertia relief technique needs to be applied [40]. The sum of forces and moments are calculated and the whole structure is fixed in a set of virtually created supports. After that, translational and rotational accelerations are applied in such a way that the reactions in these supports are close to zero. From this point, a conventional static analysis is carried out to obtain the elastic response of the structure.

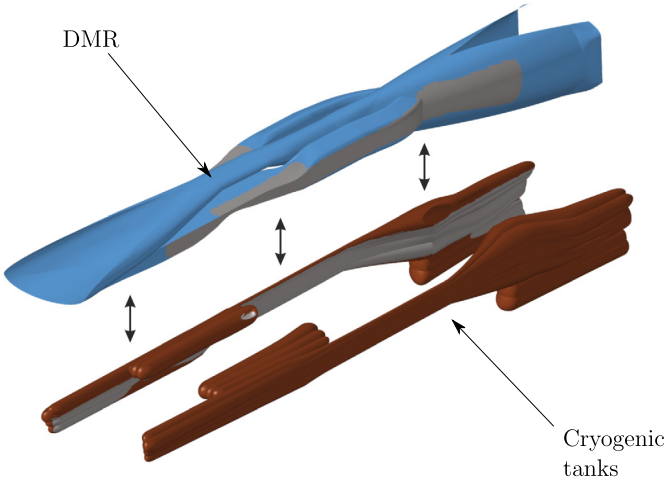

Fig. 4. Tie between the DMR and the cryogenic tanks.

In order to make a computationally efficient global model, the precise definition of the semi-monocoque scheme is replaced by an equivalent shell thickness, with the same stiffness value. Several methods have been studied [41,42] that employ a smeared stiffness approach. The one introduced by Collier [43] was used through its implementation in Hypersizer [44]. Using this approach, the detailed structure can be considered in a global model without incurring in large computational costs.

3.2. Loads

The FE model is subjected to the multidisciplinary loads summarized in Table 1. The inner pressure inside cryogenic tanks was taken as 0.5 bar (50 000 Pa), as in the LAPCAT MR2.4 [45] vehicle which allows for the correct operation of the engine. Inside the passenger cabin, a standard pressurization value of 12 psi (82 737 Pa), common in commercial aircraft, was applied.

Table 1
Load summary.

Type of load	Load	Source	Modeling
Dead	Vehicle weight	Material and thicknesses	Material density
	Passenger load	Cabin layout	Distributed load
	Landing gear	Weight	Concentrated mass
	Fuel weight	Fuel density	Hydrostatic pressure
Internal pressures	Cabin Pressurization	Standard value for commercial airplane	Uniform pressure
	Fuel Tanks pressure	Fuel pressure	Uniform pressure
External Aerodynamic	Skin aerodynamic load	CFD Analysis	Interpolated pressure
	Resultant forces on empennages	CFD Analysis	Concentrated Load
Engine Pressures	Engine inlet, combustion chamber and nozzle loads	CFD Analysis	Interpolated pressure field
Thermal	Thermal load on engine and skin	Thermal Analysis	Interpolated temperature field

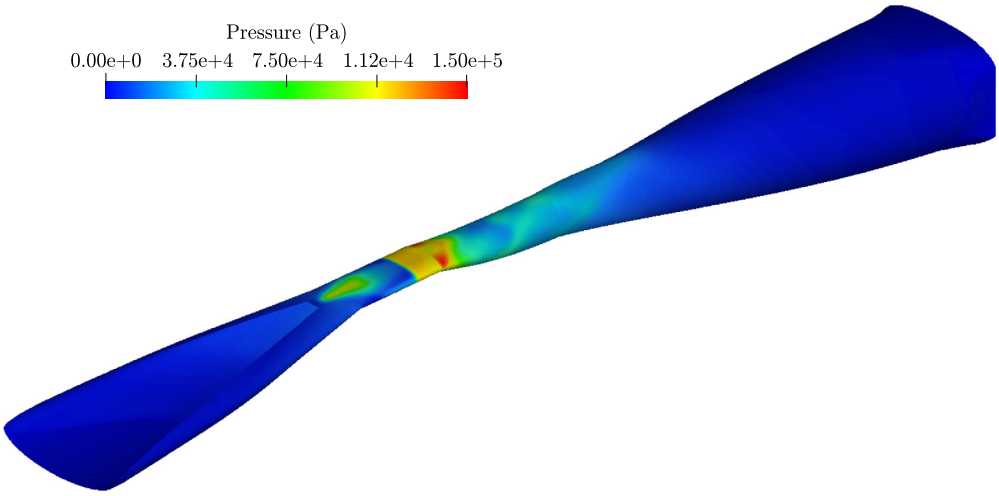

Fig. 5. Pressure distribution on the DMR obtained from CFD applied on the FEM.

To apply the aerodynamic loads, the values obtained from the CFD analysis carried out in the LAPCAT project were used [46]. Given that the FEM mesh and CFD meshes are quite different in size and element type, an adequate mapping of the nodal values from one model to the other was required. This was achieved by performing an interpolation of the nodal pressures from the CFD mesh and obtaining a full pressure field definition throughout the aircraft geometry. The application of this field to the finite element mesh provides the loads necessary to perform a stress analysis. The resulting pressures contours applied to the DMR model are shown in Fig. 5.

Regarding the thermal loads, it is critical to study multiple points in the mission trajectory to evaluate the material performance. As a result of the high velocity achieved by the vehicle, very high temperatures are reached in the leading edges, inlet and combustor ($\sim$ 2500 K), which will highly stress the materials in these areas. To input these values in the model, the temperatures coming from a thermal analysis of the LAPCAT project were applied in the same manner as the one used with the aerodynamic loads.

3.3. Materials

As previously stated, the leading edges and engine of the vehicle reach very high temperatures ($> 2500°C$), so a material capable of sustaining structural integrity at these circumstances is needed. Ceramic Matrix Composite (CMC) are composite materials consisting of ceramic fibers embedded in a ceramic matrix, forming a ceramic fiber-reinforced material. They are designed to overcome the brittleness of monolithic ceramic materials while maintaining their advantageous high temperature stability, high specific strength and stiffness. Given its high-temperatures strength and chemical inertness, it is a very favorable material to be used both in the exterior skin and in the engine [47,48]. Some experimental materials were taken into consideration: Whipox, Oxhipol and UMOX [49] but lacked some necessary features. Finally an experimental C/C-SiC composite was used whose mechanical properties are shown in Table 2.

For the cryogenic tanks, several alternatives were considered. CFRP have proven to be a plausible solution [50], but the designs are not suitable for the complex geometry of the multi-bubble STRATOFLY MR3 vehicle tanks. We found that an isotropic material capable of sustaining cryogenic temperatures behaves better in this application, so Aluminum 2195-T8 [51] has been the final material choice. Finally CFRP has been chosen for the passenger cabin, as proper insulation can be put into place to prevent the structure to reach undesirable temperatures. An effective laminate graphite/epoxy AS4/3502 with fiber percentages of 30% for 0°, 40% for 45° and 30% for 90° is used in the model.

3.4. Preliminary analysis and flaws encountered

The resulting FE model has a total of 1.6 million elements and 7.8 million degrees of freedom, customized to be used with the MSC Nastran [52] solver. In order to assess the performance of the aircraft prototype, both a stress and an eigenvalue analysis was carried out. Although a good overall structural behavior was achieved, mainly due to the inertia provided by the integral tank design, the analysis revealed some drawbacks. Those issues consists of highly loaded areas where there is little structural material,

Table 2
Material properties, elastic moduli in GPa, density in g/cm^3, thermal coefficients in μm/m · K and strength in MPa.

Material	E_1	E_2	ν_{12}	G_{12}	G_{13}	G_{23}	ρ	α	Yield strength
Aluminum 2195-T8	78.00	-	0.33	-	-	-	2.70	23.00	580
Ceramic Matrix Composite	60.00	-	0.33	-	-	-	1.90	6.50	300
AS4/3502 effective laminate	53.96	53.96	0.26	15.52	3.76	3.76	1.58	2.09	-

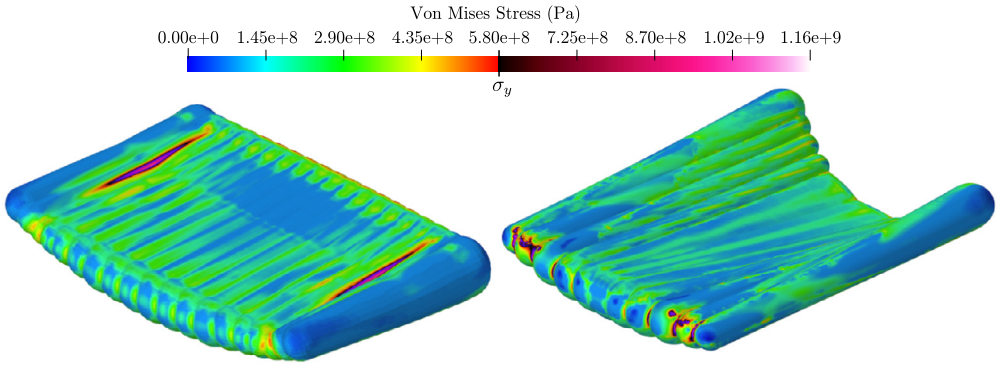

Fig. 6. Stress concentrations in cryogenic tanks.

so additional lightweight members are needed to reinforce these components.

The major flaws present in the aircraft design were related to stress concentrations in multi-bubble and engine components (Fig. 6), big displacements in the combustor, and also some local vibrational modes. Fig. 6 shows several stress concentrations in the aluminum cryogenic tanks, reaching stress levels exceeding the yield point of the material $\sigma_y = 580$ MPa.

4. Enhanced structural configurations

In this section, new concepts will be applied to the tanks and propulsion system to obtain a sound design, aiming to palliate high stress levels and local vibration modes present in some wide unstiffened areas. Three structural schemes are developed to achieve an adequate behavior of the multi-bubble components: stress relievers, bubble tension rods and lightweight structural connecting elements. The global performance was assessed afterwards through the analysis of all the components integrated into the model.

4.1. Stress relievers

The multi-bubble architecture has some limitations mainly due to the transition between the cusps of each individual lobe. At these locations a discontinuity in the load path generates stress concentrations that disrupt the membrane behavior of the component. In order to palliate this effect, thin walled shell elements were designed which provide two load paths, in vertical and horizontal planes, to eliminate the concentration of stresses. These thin wall shell elements subject to tensile forces, denoted as stress relievers, are designed following the curvature of the bubbles using smooth surfaces bonded in a cross-like shape, as shown in Fig. 7. They cover the smallest area necessary to dissipate the stresses, with approximate dimensions of 1.0 m long, 0.4 m high and 0.5 m wide.

4.2. Multi-bubble internal tension rods

In addition to the issues explained above, the multi-bubble cryogenic tanks distributed throughout the vehicle also exhibit a lack of load carrying capacity while transferring other component internal forces. Due to their size and shape, these tanks and, consequently, the aircraft are subjected to deflections that significantly alter the exterior aerodynamic profile and cause stress concentrations at the tanks edges. Thus, a structural scheme in the interior of the tanks has been devised to deal with this issue. Conceptually, such scheme will create load paths between the top and bottom faces of the bubble in order to reduce the deflections and stresses. To avoid a significant impact on tanks capacity, the new elements have to be located in the webs between bubbles. Taking into account the complex geometry of the tanks, an adequate design of these elements is far from obvious. For that reason, a slew of alternatives are considered, ranging from simple tension rods to a complete wall. In order to study them, a topology optimization study has been performed. This technique has proven to be a very valuable tool to obtain efficient designs for complex aircraft structures [53], and gives the designer the optimum material distribution in a predefined region, allowing the definition of real parts that mimic the obtained layout.

For the cryogenic tanks, the plane that divides each multi-bubble lobe is defined as the design field where material can be distributed. With this formulation, the solution can range from closed ribs that divide each region, to lighter elements that carry the loads efficiently. The technique is formulated using the Solid Isotropic Material with Penalization Method (SIMP). The objective is to minimize the compliance subject to a volume fraction constraint and stress constraints. The Sequential Quadratic Programming algorithm is selected to solve the optimization problem until the objective function tolerance, set to 10^{-4}, is reached The results of the topology optimization for the wing tanks are shown in Fig. 8. These results have to be converted into manufacturable components. To do so, an engineering interpretation is carried out, where structural elements match high density areas. Analyzing the structural layout and taking into account that the designed elements will work exclusively under tensile forces in a static analysis, a set of tension bars is chosen as the most suitable solution. These tension rods are arranged in each design region with a wide variety of angles, in some cases even defining crossing configurations.

4.2.1. Lightweight structural elements connecting volumes of the vehicle

Three different structural schemes have been developed to join different parts of the vehicle with a minimum weight increment: DMR combustor, rear cryogenic tank and passenger cabin.

Among the plethora of technical issues tackled in the design of this aircraft, designing a stable air-breathing high-speed combustion system is of paramount importance. For the correct operation

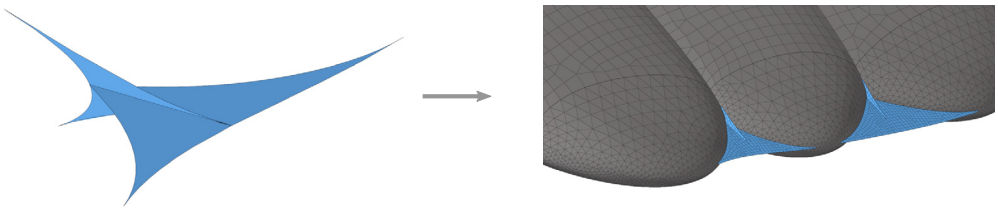

Fig. 7. Stress relievers for multi-bubble concepts.

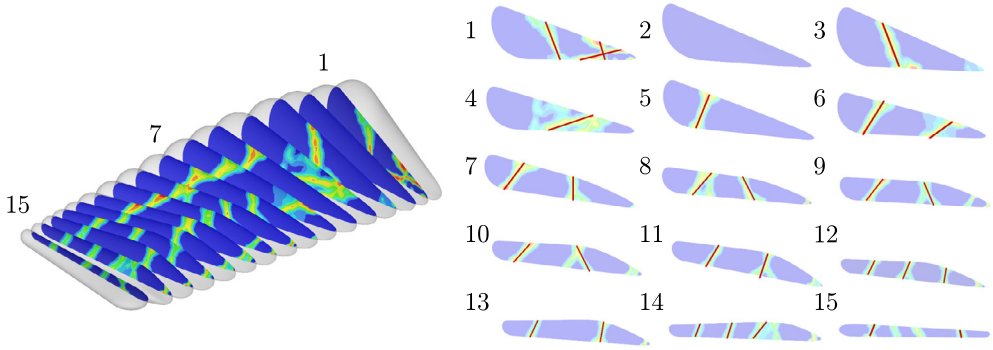

Fig. 8. Topology Optimization and structural realization of the cryogenic wing tanks.

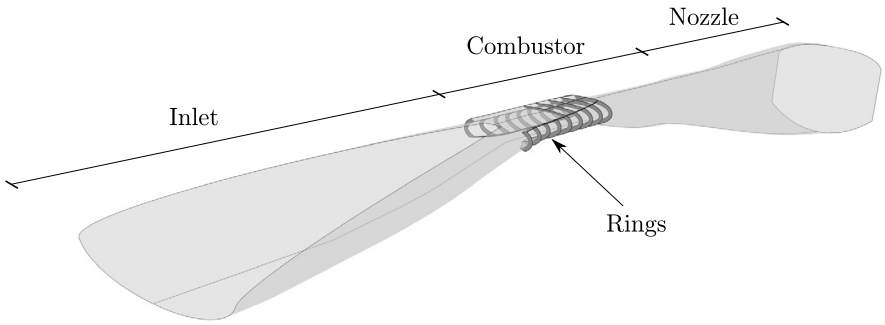

Fig. 9. Open rings location in the DMR engine.

of the DMR engine of the STRATOFLY MR3 vehicle the combustor must undergo very small deformations. The high temperatures and pressures reached during the combustion result in high displacements that alter the designed flow path. To avoid the above situation, an assembly of incomplete elliptical rings, shown in Fig. 9, was designed to maximize the strength of the component while allowing the deployment of low speed flow path doors, that are located specifically below the combustor.

Apart from the aforementioned issues addressed with stress relievers and tension rods, another problem in the rear cryogenic tank is related to the connectivity with its surrounding components (DMR nozzle and DMR surrounding tank). To connect the volumes, planar surfaces within the gap between them could be perfectly fitted, but the sharp geometry would produce local stress concentrations. For that reason, a set of ribs with smooth transitions were adopted, following the bisector planes between the bubbles (Fig. 10). In this way, they are able to carry the loads without introducing any undesirable effects.

Finally, for the passenger cabin, another grillage was designed taking into account the same idea. Fig. 11 shows the set of elements that connect above with the DMR and below with the exterior skin. To complete the structural configuration, tension rods were positioned inside the cabin, anchored at the top and bottom rib elements, maintaining enough distance between them to allow for the distribution of passengers in several aisles. This idea was also implemented in the D8 Double-Bubble fuselage [54] designed by Aurora Sciences, where the tension rods are anchored to a keel beam that is located between the two lobes of the fuselage.

5. Results and discussion

Once the new structural schemes were developed and introduced in the FE model, a static analysis of the full vehicle is performed to evaluate the mechanical performance. Results are presented in Table 3, showing the zones where the material reaches the failure criteria and the maximum displacements for each load case. We can observe that during climb, at Mach 0.5 and Mach 0.75, the aerodynamic pressure is maximum and a greater percentage of the material violates the failure criteria. However, all the values obtained are below 1% of the total structure area, which denotes an adequate performance at this stage of the design.

Concerning the general stiffness, the biggest displacements are at the nozzle top location. This outcome comes as a result of the engine nozzle size, which has over 10 meters in diameter, larger than any other ever built for a propulsion system. This geometrical characteristic, combined with the pressures and temperatures coming from the exhaust gases, make this area critical. The external and internal aerodynamics cannot be disrupted in the rear part of the vehicle, so no additional volumes that strengthen the area using integral tanks is plausible. However, this values are within the required operational limits, and do not significantly disrupt the airflows during the mission.

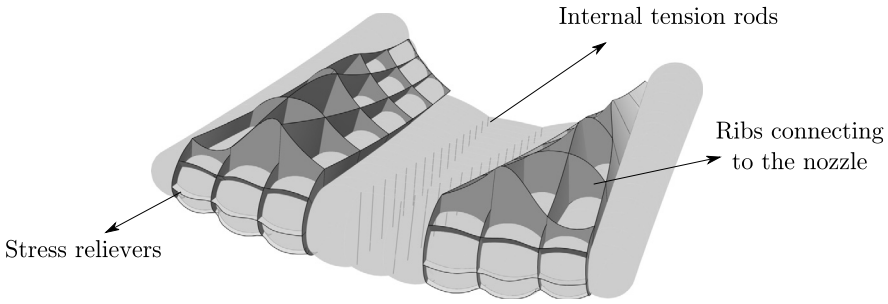

Fig. 10. Rear cryogenic tank.

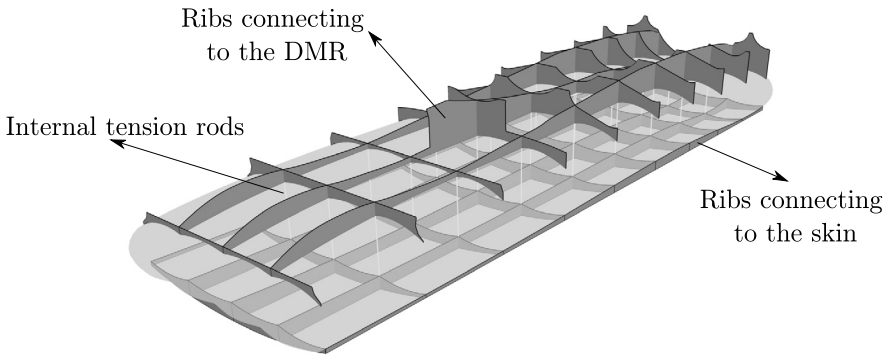

Fig. 11. Passenger cabin structural layout.

Table 3
Global models results. AoA stands for angle of attack. Displacements in m.

Load Case		Material area	Displacement	
Mach	AoA	violating failure criteria	Max Value	Area
0.5	-2.0°	0.94%	0.337	Nozzle top
	0.0°	-	-	-
	2.0°	0.95%	0.335	Nozzle top
0.75	-2.0°	-	-	-
	0.0°	0.15%	0.221	Nozzle top
	2.0°	-	-	-
4	-2.0°	0.07%	0.168	Cabin bottom
	0.0°	0.08%	0.167	
	2.0°	0.07%	0.167	
6	-2.0°	0.08%	0.164	Cabin bottom
	0.0°	0.09%	0.164	
	2.0°	0.08%	0.168	
8	-2.0°	0.08%	0.122	Cabin bottom
	0.0°	0.10%	0.168	
	2.0°	0.09%	0.135	

Fig. 12 shows the displacements contour for the complete vehicle during cruise at 0 degrees angle of attack and Mach 8 speed, i.e. the nominal cruise condition. The results show very low relative displacement in most components of the aircraft, which make it possible to maintain the exterior aerodynamic surfaces and the internal flowpaths working in an efficient manner. This shows the effectiveness of the improved structural schemes with: the addition of tension rods in the tanks, the stiffening rings around the combustor, the grillage in the rear tank and the passengers cabin, and the stress relievers.

A similar effect can be seen if material strength is considered. In order to plot the performance of all the materials simultaneously, a margin of safety plot has been defined. The margin of safety is defined as the surplus of the allowable value with regards to the results obtained for the conditions studied. For the aluminum and CMC the yield stress is considered the allowable magnitude and for CFRP the maximum strain criteria. Fig. 13 shows that for cruise (Mach 8 and 0 degrees of angle of attack) high margins are present in the inlet and nozzle, while the most demanding areas correspond to the fuselage tanks and some spots between the bubbles of the wing tanks. To further analyze this critical areas, a more detailed FEM should be used to further refine this structural details.

As shown in Fig. 14 the structural layout on the DMR combustor has achieved an outstanding performance. The longitudinal local peak values of the displacements and stresses have been resolved with the addition of the incomplete set of rings, which added a minimum penalty weight to the structure. The flow paths is maintained and the structure is able to resist and redistribute the loads coming from the internal pressures and temperatures.

Furthermore, the effect of the stress relievers solved the issues in the bubble transitions. Fig. 15 depicts the phenomenon. In the original design, a stress buildup was present due to the non-smooth changes in curvature. After the inclusion of the stress reliever device, the new load path dissipates the stresses so they do not reach the yield point of the material.

We set up these elements throughout the wing and fuselage tanks. The weight penalty was low for the large volumes but relatively high in the small high-curvature ones. These findings and the superior volumetric efficiency argue favorably for the high-dimension bubbles inclusion in an integral tank design.

Fig. 16 compares the stress levels in the wing tanks surface with three different approaches: without considering tension rods, using a preliminary design with parallel vertical rods along each design region, and incorporating the engineered tension rods obtained from the topology optimization. It can be seen that the two latter schemes solve the problem, but only the one extracted from the optimization does not create additional stress concentrations. Overall, the weight added by all the elements incorporated in the design (rings, stress relievers and other lightweight structural elements) amounts to 2.8% of the total structural weight.

The first natural frequency of the vehicle occurs at 7.28 Hz, and the first 10 are below 12 Hz. Although some local modes are

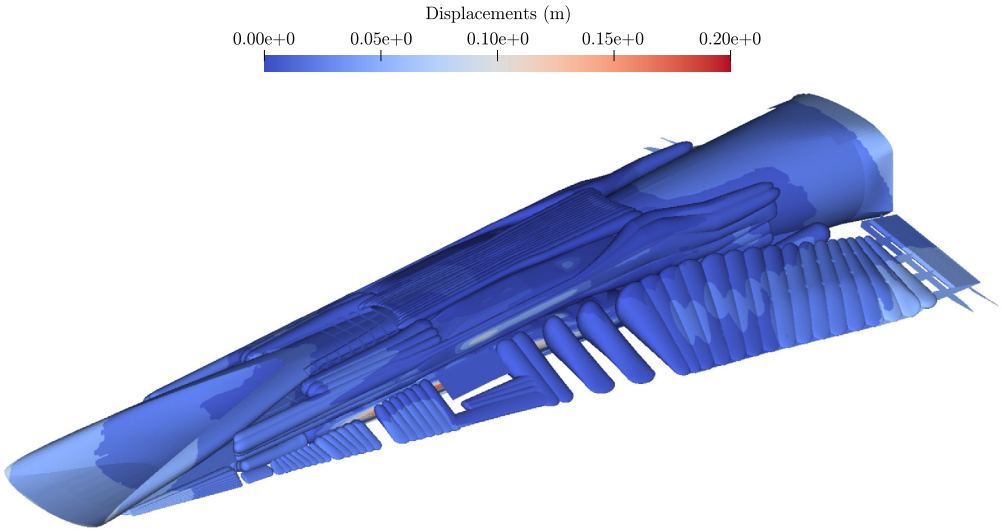

Fig. 12. Global displacements.

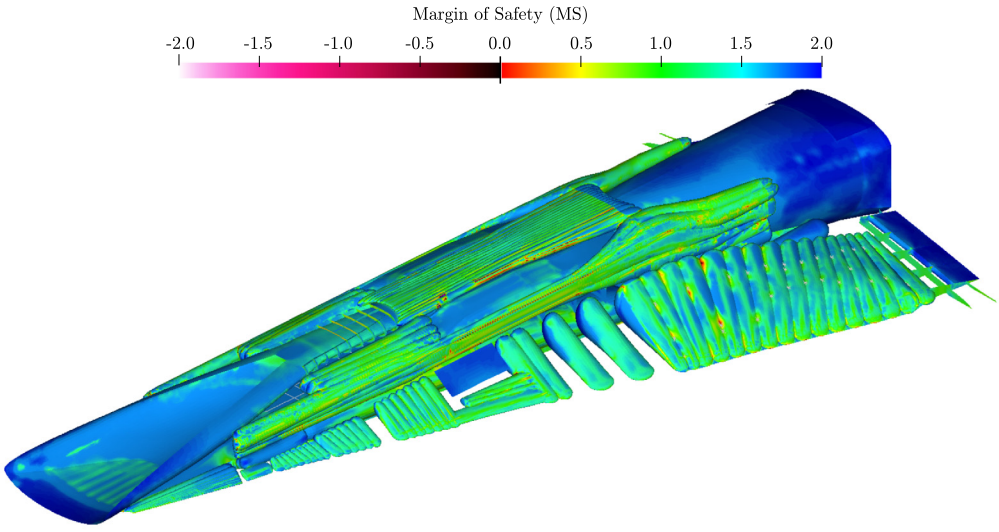

Fig. 13. Global stresses.

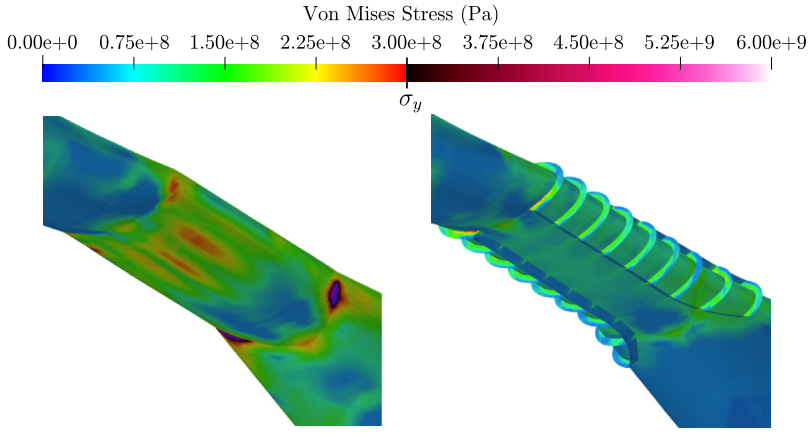

Fig. 14. Stress mitigation in the DMR combustor.

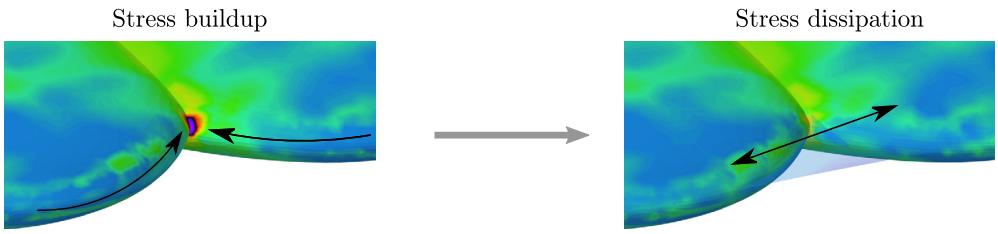

Fig. 15. Stress relievers effect on the bubble cusps.

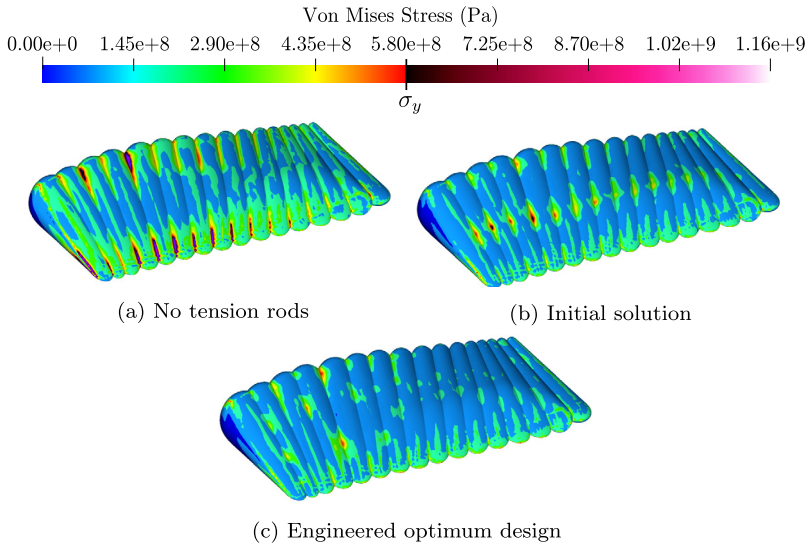

Fig. 16. Comparison between the different tension rods solutions.

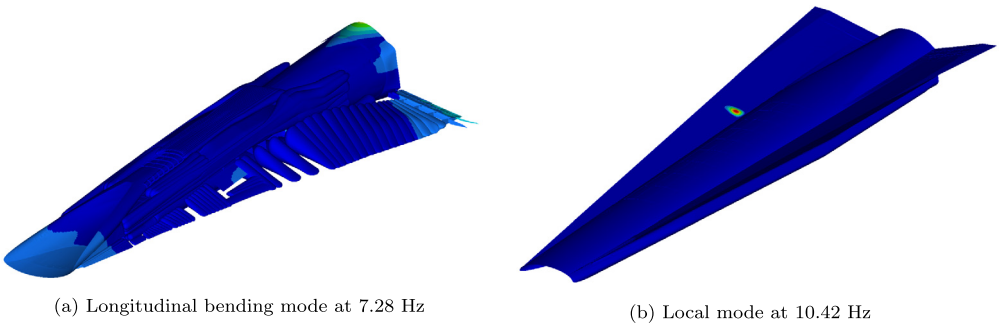

Fig. 17. Eigenmode analysis of the vehicle.

present, the bulk of the mass participation factors is carried out by the global ones. Fig. 17 shows some of the modal shapes. Particularly, Fig. 17b reveals the weak areas at the wing entrances of the vehicle, where the lack of integral tanks should be replaced by the required structural elements to avoid resonance issues during flight. The remaining modes are global vibration modes including torsion, longitudinal and lateral bending.

The sizing was obtained using a Fully Stressed Design (FSD) cycle, until a maximum yield-stress area is reached. This technique results in a lightweight design capable of sustaining all the required loads. In addition it serves as a good starting point for the upcoming optimizations that will be carried out. The mass breakdown of the MR3 vehicle is shown in Table 4, which amounts to 301.39 t of total structural mass. The heaviest components are the cryogenic tanks, accounting for 43.7% of the total weight. The weight fraction of the OML reaches 28.9%, 17.22% for the propulsion system, and 10.19% for the passengers cabin.

6. Conclusions

We have studied the STRATOFLY MR3 vehicle and designed its preliminary structural configuration. We have shown that a GFEM accurately predicts the overall structural response under the influence of multidisciplinary loads. The analyses have proven the multi-bubble concept as an efficient solution for the cryogenic tanks and passenger cabin, providing a integral architecture capable of sustaining the hypersonic loads considered. The caveats present in the design were solved by a set of structural components, achieving a sound lightweight structural scheme. Among the solutions adopted, topology optimization was a suitable technique

Table 4
Mass breakdown of the MR3 vehicle structure (dry mass).

		Thickness (mm)	Area (m^2)	Material	Weight (t)
Passengers Cabin	Skin	15	1,029.9	CFRP	24.07
	Ribs	11	387.1	CFRP	6.63
DMR	Inlet	12	399.8	CMC	9.12
	Combustor	12	94.9	CMC	2.16
	Nozzle	11	1,209.1	CMC	25.27
	Rings	12	30.9	CMC	1.05
ATR	Skin	7	1,074.6	CMC	14.29
OML	Wing bottom	8	1,122.4	CMC	17.06
	Wing top	9	1,454.5	CMC	23.49
	Fuselage bottom	9	1,269.0	CMC	21.70
	Fuselage nose	11	307.9	CMC	6.43
	Fuselage tail	9	570.6	CMC	9.76
	Fuselage center	8	573.1	CMC	8.71
Wing Tanks	Skin	12	1,820.0	Aluminium	56.51
	Stress Relievers	18	6.2	Aluminium	0.30
DMR Top Tanks	Inner Skin	12	266.6	Aluminium	8.64
	Outer Skin	11	90.7	Aluminium	2.69
DMR Side Tanks	Inner Skin	9	1,079.1	Aluminium	26.22
	Outer skin	11	240.6	Aluminium	7.15
Rear Tank	Skin	8	584.4	Aluminium	12.62
	Ribs	10	128.2	Aluminium	3.46
Inlet Tank	Skin	10	356.3	Aluminium	9.62
Front Tank	Skin	7	235.1	Aluminium	4.44
Total					301,39

to design an internal configuration for the cryogenic multi-bubble tanks.

Declaration of competing interest

The authors declare that they have no known competing financial interests or personal relationships that could have appeared to influence the work reported in this paper.

Acknowledgements

This project has received funding from the STRATOFLY Horizon 2020 research project, under grant agreement No 769246. The project has been coordinated by Politecnico di Torino and Von Karman Institute for Fluid Dynamics. In addition, the research leading to these results has been conducted under Grant PID2019-108307RB-I00 funded by MCIN/AEI/10.13039/501100011033. The authors also acknowledge funding received from the Galician Government through research grant ED431C 2017/72.

References

[1] K.M. Sayler, Hypersonic Weapons: Background and Issues for Congress, Congressional Research Service R45811.
[2] D. Sziroczak, H. Smith, A review of design issues specific to hypersonic flight vehicles, Prog. Aerosp. Sci. 84 (2016) 1–28, https://doi.org/10.1016/j.paerosci.2016.04.001.
[3] J.J. McNamara, P.P. Friedmann, Aeroelastic and aerothermoelastic analysis of hypersonic vehicles: current status and future trends, in: 14th AIAA/AHI Space Planes and Hypersonic Systems and Technologies Conference, American Institute of Aeronautics and Astronautics, Canberra, Australia, 2006.
[4] R.T. Voland, L.D. Huebner, C.R. McClinton, X-43A hypersonic vehicle technology development, Acta Astronaut. 59 (1) (2006) 181–191, https://doi.org/10.1016/j.actaastro.2006.02.021.
[5] J. Hank, J. Murphy, R. Mutzman, The X-51A Scramjet Engine Flight Demonstration Program, in: 15th AIAA International Space Planes and Hypersonic Systems and Technologies Conference, American Institute of Aeronautics and Astronautics, Dayton, Ohio, 2008.
[6] A. Kuranov, V. Kuchinsky, E. Sheikin, Scramjet with MHD control under "Ajax" concept - requirements for MHD systems, in: 32nd AIAA Plasmadynamics and Lasers Conference, American Institute of Aeronautics and Astronautics, Anaheim, CA, U.S.A., 2001.
[7] M.K. Smart, N.E. Hass, A. Paull, Flight data analysis of the HyShot 2 scramjet flight experiment, AIAA J. 44 (10) (2006) 2366–2375, https://doi.org/10.2514/1.20661.
[8] J. Steelant, ATLLAS: aero-thermal loaded material investigations for high-speed vehicles, in: 15th AIAA International Space Planes and Hypersonic Systems and Technologies Conference, American Institute of Aeronautics and Astronautics, Dayton, Ohio, 2008.
[9] J. Steelant, T. Langener, The LAPCAT-MR2 hypersonic cruiser concept, in: 29th Congress of the International Council of the Aeronautical Sciences, ICAS, St. Petersburg, Russia, 2014.
[10] E. Blanvillain, G. Gallic, HIKARI: paving the way towards high speed air transport, in: 20th AIAA International Space Planes and Hypersonic Systems and Technologies Conference, American Institute of Aeronautics and Astronautics, Glasgow, Scotland, 2015.
[11] J. Steelant, T. Langener, F. Di Matteo, K. Hannemann, J. Riehmer, M. Kuhn, C. Dittert, F. Scheuerpflug, W. Jung, M. Marini, G. Pezzella, M. Cicala, L. Serre, Conceptual design of the high-speed propelled experimental flight test vehicle HEXAFLY, in: 20th AIAA International Space Planes and Hypersonic Systems and Technologies Conference, 2015.
[12] G. Pezzella, M. Marini, B. Reimann, J. Steelant, Aerodynamic design analysis of the HEXAFLY-INT hypersonic glider, in: 20th AIAA International Space Planes and Hypersonic Systems and Technologies Conference, Glasgow, Scotland, 2015.
[13] Stratospheric flying opportunities for high-speed propulsion concepts, in: Topic: MG-1-4-2016-2017 - Breakthrough innovation STRATOFLY, European Comission Horizon 2020, 2017.
[14] N. Viola, R. Fusaro, B. Saracoglu, C. Schram, V. Grewe, J. Martinez, M. Marini, S. Hernanzed, K. Lammers, A. Vincent, D. Hauglustaine, B. Liebhardt, F. Linke, C. Fureby, Main challenges and goals of the H2020 STRATOFLY project, in: International Conference on Flight Vehicles, Aerothermodynamics and Re-Entry Missions & Engineering, FAR, 2019.
[15] A. Beachy, H. Bae, I. Boyd, R. Grandhi, Emulator embedded neural networks for multi-fidelity conceptual design exploration of hypersonic vehicles, Struct. Multidiscip. Optim. (2021), https://doi.org/10.1007/s00158-021-03005-y.
[16] Z.-t. Zhao, W. Huang, L. Yan, Y.-g. Yang, An overview of research on wide-speed range waverider configuration, Prog. Aerosp. Sci. 113 (2020) 100606, https://doi.org/10.1016/j.paerosci.2020.100606.
[17] M.K.L. O'Neill, M.J. Lewis, Design tradeoffs on scramjet engine integrated hypersonic waverider vehicles, J. Aircr. 30 (6) (1993) 943–952, https://doi.org/10.2514/3.46438.

[18] M. Ardema, Structural weight analysis of hypersonic aircraft, Technical Report TN D-6692, NASA, 1972.
[19] M. Ardema, E. Terjesen, C. Roberts, Body weight of advanced concept hypersonic aircraft, in: Aircraft Design and Operations Meeting, Aircraft Design and Operations Meetings, American Institute of Aeronautics and Astronautics, 1991.
[20] M.D. Ardema, Structural sizing for buckling critical body structure of advanced aircraft, J. Aircr. 40 (6) (2003) 1208–1211, https://doi.org/10.2514/2.7213.
[21] B.M. Yutko, N. Titchener, C. Courtin, M. Lieu, L. Wirsing, J. Tylko, C.T. Jeffrey, T.W. Roberts, C.S. Church, Conceptual design of a D8 commercial aircraft, in: 17th AIAA Aviation Technology, Integration, and Operations Conference, American Institute of Aeronautics and Astronautics, Denver, Colorado, 2017.
[22] M. Drela, Development of the D8 transport configuration, in: 29th AIAA Applied Aerodynamics Conference, American Institute of Aeronautics and Astronautics, Honolulu, Hawaii, 2011.
[23] R.H. Liebeck, Design of the blended wing body subsonic transport, J. Aircr. 41 (1) (2004) 10–25, https://doi.org/10.2514/1.9084.
[24] C. Meerts, J. Steelant, Air Intake Design for the Acceleration Propulsion Unit of the LAPCAT-MR2 Hypersonic Aircraft, 2013.
[25] T. Zhang, Z. Wang, W. Huang, D. Ingham, L. Ma, M. Porkashanian, An analysis tool of the rocket-based combined cycle engine and its application in the two-stage-to-orbit mission, Energy 193 (2020) 116709, https://doi.org/10.1016/j.energy.2019.116709.
[26] W. Beaulieu, R. Campbell, W. Burcham, Measurement of XB-70 propulsion performance incorporating the gas generator method, J. Aircr. 6 (4) (1969) 312–317, https://doi.org/10.2514/3.44057.
[27] W. Huang, Z.-b. Du, L. Yan, Z.-x. Xia, Supersonic mixing in airbreathing propulsion systems for hypersonic flights, Prog. Aerosp. Sci. 109 (2019) 100545, https://doi.org/10.1016/j.paerosci.2019.05.005.
[28] W. Huang, Z.-b. Du, L. Yan, R. Moradi, Flame propagation and stabilization in dual-mode scramjet combustors: a survey, Prog. Aerosp. Sci. 101 (2018) 13–30, https://doi.org/10.1016/j.paerosci.2018.06.003.
[29] T. Zhang, X. Yan, W. Huang, X. Che, Z. Wang, Multidisciplinary design optimization of a wide speed range vehicle with waveride airframe and RBCC engine, Energy 235 (2021) 121386, https://doi.org/10.1016/j.energy.2021.121386.
[30] M. Lobbia, K. Suzuki, Multidisciplinary design optimization of hypersonic transport configurations using waveriders, in: 19th AIAA International Space Planes and Hypersonic Systems and Technologies Conference, American Institute of Aeronautics and Astronautics, Atlanta, GA, 2014.
[31] N. Murray, J. Steelant, A. Mack, Conceptual design of a Mach 8 hypersonic cruiser with dorsal engine, in: Sixth European Symposium on Aerothermodynamics for Space Vehicles, Versailles, France, 2008, p. 8.
[32] K.D. Jones, H. Sobieczky, A.R. Seebass, F.C. Dougherty, Waverider design for generalized shock geometries, J. Spacecr. Rockets 32 (6) (1995) 957–963, https://doi.org/10.2514/3.26715.
[33] T. Zhang, X. Yan, W. Huang, X. Che, Z. Wang, E. Lu, Design and analysis of the air-breathing aircraft with the full-body wave-ride performance, Aerosp. Sci. Technol. 119 (2021) 107133, https://doi.org/10.1016/j.ast.2021.107133.
[34] I. Cumalioglu, A. Ertas, Y. Ma, T. Maxwell, State of the art: hydrogen storage, J. Fuel Cell Sci. Technol. 5 (3) (2008) 034001, https://doi.org/10.1115/1.2894462.
[35] D. Glass, Ceramic Matrix Composite (CMC) Thermal Protection Systems (TPS) and hot structures for hypersonic vehicles, in: 15th AIAA International Space Planes and Hypersonic Systems and Technologies Conference, American Institute of Aeronautics and Astronautics, Dayton, Ohio, 2008.
[36] A.N.A. Dasgupta, Fluid-Thermal-Structural Interactions on a Fin in Hypersonic Flow, Melbourne, Australia, 2014.
[37] N. Viola, R. Fusaro, O. Gori, M. Marini, P. Roncioni, G. Saccone, B. Saracoglu, A. Ispir, C. Fureby, T. Nilsson, C. Ibron, N. Zettervall, K. Bates, A. Vincent, J. Martinez-Schram, V. Grewe, J. Pletzer, D. Hauglustaine, F. Linke, D. Bodmer, Stratofly mr3 – how to reduce the environmental impact of high-speed transportation, in: AIAA Scitech 2021 Forum, 2021, pp. 1–21.
[38] J. Steelant, R. Varvill, S. Defoort, K. Hannemann, M. Marini, Achievements obtained for sustained hypersonic flight within the lapcat-ii project, in: 20th AIAA International Space Planes and Hypersonic Systems and Technologies Conference, Glasgow, Scotland, 2015.
[39] Altair inc., Altair Hypermesh: High-fidelity Finite Element Modeling, 2019.
[40] L. Liao, A study of inertia relief analysis, in: Collection of Technical Papers - AIAA/ASME/ASCE/AHS/ASC Structures, Structural Dynamics and Materials Conference, 2011.
[41] J.M. Hedgepeth, D.B. Hall, Stability of stiffened cylinders, AIAA J. 3 (12) (1965) 2275–2286, https://doi.org/10.2514/3.3357.
[42] Y. Xia, M.I. Friswell, E.I.S. Flores, Equivalent models of corrugated panels, Int. J. Solids Struct. 49 (13) (2012) 1453–1462, https://doi.org/10.1016/j.ijsolstr.2012.02.023.
[43] C. Collier, Thermoelastic formulation of stiffened, unsymmetric composite panels for finite element analysis of high speed aircraft, in: 35th Structures, Structural Dynamics, and Materials Conference, American Institute of Aeronautics and Astronautics and Head, SC U. S. A, Hilton, 1994.
[44] Collier Research corporation, Hypersizer, 2018.
[45] J. Steelant, M. van Duijn, Structural analysis of the LAPCAT-MR2 waverider based vehicle, in: 17th AIAA International Space Planes and Hypersonic Systems and Technologies Conference 2011, 2011.
[46] P. Roncioni, P. Natale, M. Marini, T. Langener, J. Steelant, Numerical simulations and performance assessment of a scramjet powered cruise vehicle at Mach 8, Aerosp. Sci. Technol. 42 (2015) 218–228, https://doi.org/10.1016/j.ast.2015.01.006.
[47] M. Bouchez, E. Dufour, B. Le Naour, C. Wilhelmi, K. Bubenheim, M. Kuhn, B. Mainzer, J. Riccius, C. Davoine, J.F. Justin, M. Axtmann, J. von Wolfersdorf, S. Spring, V.F. Villace, J. Steelant, Combustor materials research studies for high speed aircraft in the european program ATLLAS-II, in: 20th AIAA International Space Planes and Hypersonic Systems and Technologies Conference, Glasgow, Scotland, 2015.
[48] J. Steelant, Achievements obtained on aero-thermal loaded materials for high-speed atmospheric vehicles within ATLLAS, in: 16th AIAA/DLR/DGLR International Space Planes and Hypersonic Systems and Technologies Conference, Bremen, Germany, 2009.
[49] E. Volkmann, K. Tushtev, D. Koch, C. Wilhelmi, J. Göring, K. Rezwan, Assessment of three oxide/oxide ceramic matrix composites: mechanical performance and effects of heat treatments, Composites, Part A, Appl. Sci. Manuf. 68 (Jan. 2015), https://doi.org/10.1016/j.compositesa.2014.09.013.
[50] M. Sippel, A. Kopp, D. Mattsson, Final results of advanced cryo-tanks research project CHATT, in: 6th European Conference for Aeronautics and Space Sciences (EUCASS), Krakow, Poland, 2015.
[51] N. Nayan, S.V.S. Narayana Murty, A.K. Jha, B. Pant, S.C. Sharma, K.M. George, G.V.S. Sastry, Mechanical properties of aluminium–copper–lithium alloy AA2195 at cryogenic temperatures, Mater. Des. 58 (2014) 445–450, https://doi.org/10.1016/j.matdes.2014.02.024.
[52] Msc software, MSC Nastran: Multidisciplinary Structural Analysis, 2019.
[53] N. Aage, E. Andreassen, B.S. Lazarov, O. Sigmund, Giga-voxel computational morphogenesis for structural design, Nature 550 (7674) (2017) 84–86, https://doi.org/10.1038/nature23911.
[54] J.T. Chambers, B.M. Yutko, R. Singh, C. Church, Structural optimization study of the D8 double-bubble composite fuselage, in: 58th AIAA/ASCE/AHS/ASC Structures, Structural Dynamics, and Materials Conference, Grapevine, Texas, 2017.